Accepted Manuscript

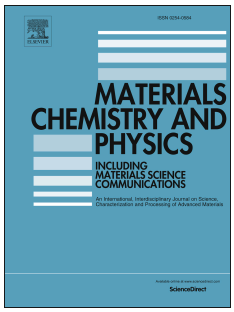

Design of carbon nanofiber embedded conducting epoxy resin

Subhra Gantayat, Niladri Sarkar, Dibyaranjan Rout, Sarat K. Swain

PII: S0254-0584(16)30683-6

DOI: 10.1016/j.matchemphys.2016.09.020

Reference: MAC 19166

To appear in: *Materials Chemistry and Physics*

Received Date: 19 March 2016

Revised Date: 5 September 2016

Accepted Date: 10 September 2016

Please cite this article as: S. Gantayat, N. Sarkar, D. Rout, S.K. Swain, Design of carbon nanofiber embedded conducting epoxy resin, *Materials Chemistry and Physics* (2016), doi: 10.1016/j.matchemphys.2016.09.020.

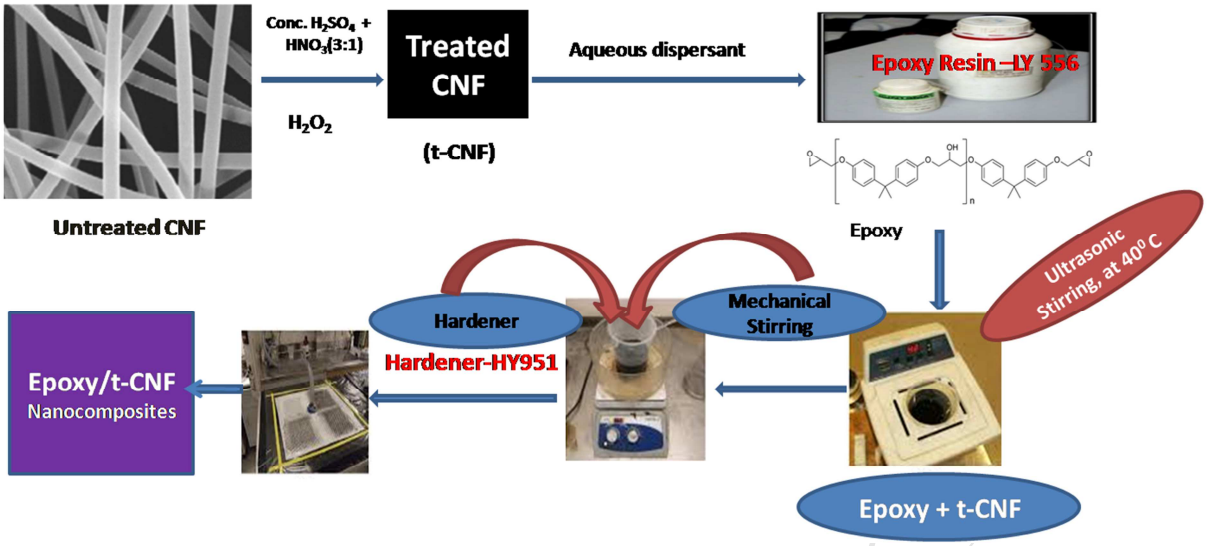

Design of carbon nanofiber embedded conducting epoxy resin

Subhra Gantayat[1, 2], Niladri Sarkar[1], Dibyaranjan Rout[2], Sarat K. Swain*[1]
[1]Department of Chemistry, Veer Surendra Sai University of Technology, Burla, Sambalpur-768018, Odisha, India
[2]School of Applied Sciences, KIIT University, Bhubaneswar-751024, Odisha, India
*Corresponding author: Email: swainsk2@yahoo.co.in Phone: 91-9937082348, Fax: 91-663-2430204

Abstract

Acid treated carbon nanofiber (t-CNF) reinforced epoxy nanocomposites were fabricated by hand lay-up method with various wt % of t-CNF loadings. Pristine or unmodified carbon nano fibers (u-CNFs) were made compatible with epoxy matrix by means of mixed acid treatment. Fabricated nanocomposites were characterized with Fourier transform infrared spectroscopy (FTIR), X-ray diffraction (XRD) study, scanning electron microscopy (SEM), transmission electron microscopy (TEM) and atomic force microscopy (AFM). Mechanical and thermal properties of the nanocomposites were measured as a function of t-CNF content. Effect of acid treated CNFs on to the mechanical properties of epoxy nanocomposites was justified by comparing the mechanical properties of epoxy/t-CNF and epoxy/u-CNF nanocomposites with same loading level. The electrical conductivity was achieved by epoxy resin with a threshold at 1 wt % of t-CNF. Substantial improvement in thermal, mechanical and electrical properties of the synthesized epoxy/t-CNF nanocomposites may be suitable for fabricating electronic devices.

Keywords: Carbon nanofiber (CNF)**;** Atomic force microscopy (AFM); Fourier transforms infrared spectroscopy (FTIR); Scanning electron microscopy (SEM); Thermogravimetric Analysis (TGA)

Introduction

After the discovery of carbon fibers (CFs) from the carbonization of cotton and bamboo in 1879 and its application as filament materials, carbon fiber based composites have gained momentum in the fields of fundamental scientific research and practical applications [1-4]. Nano-scaled fillers such as carbon nanotubes (CNT) and carbon nanofibers (CNF) offer new possibilities towards low-weight composites with extraordinary mechanical, electrical, and thermal properties. Recently, nano carbon filled epoxy composites have drawn a great deal of attention owing to their potential applications in automotive, aeronautics, marine industry and electronics. Moreover, carbon nanofiber reinforced polymer nanocomposites have also been used for energy conversion, energy storage and self-sensing applications [5-8]. Now-a-days, researchers are also trying to fabricate hetero-atom doped carbon nanofibers (DCNFs) for the development of high-quality supercapacitors [9, 10]. Carbon nanotubes (CNTs) are well known potential filler for epoxy nanocomposites with smaller dimension, lower density and micro-structural defects, but these are expensive. Functionalization or chemical modification of CNTs can induce nanotube damage and van der Waals forces can drive the nanotube to form ropes or reassemble after being dispersed. In this context, carbon nano fibers (CNFs) are cost effective, can be produced at high yields and are also less affected by van der Waals forces as a result they can stay dispersed for longer period of time [11, 12]. Carbon nanofibers with an average diameter of 100-200 nm and fiber length of ≈30-50μm provide high aspect ratio by which it can withstand a load of 2kg whereas; a steel wire of the same thickness endures only 200g [13]. Additionally, CNFs exhibit adequate physical properties i.e. conductivity (electrical ≈10^3 S/cm, thermal ≈1900 $wm^{-1}K^{-1}$) and mechanical properties (Young's modulus ≈ 500G Pa, tensile strength ≈ 3G Pa) [14]. As far as polymer matrix is concerned, epoxy resins are considered to be

well established thermosetting matrices exhibiting a list of interesting properties such as high stiffness, high strength, dimensional stability, chemical resistance and strong adhesion to the embedded reinforcement [15].

Hence, there has been an up-growing interest among the new generation researchers for the study of advanced composites with the different allotropic forms of carbon and epoxy resin [16-19]. In order to achieve a well dispersed phase of carbon nanofibers (CNFs) within hot polymer matrix, different fabrication techniques have been adopted by different researchers [13, 20-21] and a partial success in improving various properties of epoxy/CNF nanocomposites has been achieved [22-25]. Choi et al. [21] has observed a maximum tensile strength of CNF/epoxy nanocomposite at 5wt % of CNF whereas; Zhou et al. [25] and Sun et al. [12] have obtained maximum tensile strength at 2 and 1.0 wt % of CNF respectively. Similarly, Sun et al. [12] has reported a significant increment in electrical conductivity by a magnitude of four to ten orders with changing the CNF content from 0.1 to 1wt % whereas; Zhu et al. [26] observed eight orders of magnitude change for epoxy nanocomposites with 0.1 to 1wt % u-CNF loadings. A very low percolation threshold of 0.064 wt % CNF is obtained by Allaoui et al. [14]. Substantial amount of work has already been done on epoxy/CNF nanocomposites, but the utilization of epoxy (LY-556) as matrix is rare in the literature.

In this present work, t-CNF reinforced epoxy nanocomposites were prepared by simple fabrication method with various wt % of t-CNF loadings (0.5, 1, 2, 3 and 4wt %). Pristine or unmodified CNF (u-CNF) is nonpolar carbon allotrope, whereas; epoxy is a polar thermosetting polymer. The compatibility of nonpolar filler like CNF and polar matrix like epoxy is a challenge for making epoxy nanocomposites with improved properties. Herein, u-CNF is chemically modified to achieve the polar nature with substitution of organic functional groups. Hence, the

modified CNF (t-CNF) is more compatible with strong interfacial adhesion for epoxy resin. Different techniques such as X-ray diffraction (XRD), scanning electron microscopy (SEM) and transmission electron microscopy (TEM) were used to characterize the epoxy/t-CNF nanocomposites. Mechanical, electrical and thermal properties of the nanocomposites were measured as a function of t-CNF content.

2. Experimental

2.1. Materials

For preparation of the composites, carbon nanofibers with (≥ 96% pure) outer diameter of 500 nm and fiber length of 600-900 nm was obtained from Intelligent Materials Pvt. Ltd, NANOSHEL LLC, USA . The epoxy resin (LY 556, Bisphenol Diglycidyl ether, Merck, India) and hardener or curing agent (HY 951, aliphatic amine, Merck, India) were purchased and used as starting materials. Araldite LY-556 is an anhydride-cured, low viscous matrix system with extremely long pot life. It is easy to process and it has good fiber impregnation properties along with excellent thermal, mechanical and rheological properties. Concentrated sulphuric acid (H_2SO_4), concentrated nitric acid (HNO_3) were of analytical grade reagents (AR) and used as such without any further purification.

2.2. Acid treatment of CNFs

Carbon nanofibers (CNFs) have a strong tendency to agglomerate due to their nano size and their respective high surface energy. However, the grafting of chemical functionalities on the CNT surface, such as carboxylates, imparts negative charges and, therefore, creates the

electrostatic stability required for a colloidal dispersion. Neat or unmodified CNFs (u-CNFs) were added to a mixture of conc. H_2SO_4 and HNO_3 in a volume ratio of 3:1 and were sonicated for 24 hr at 40 ^oC. Using distilled water, the mixture was diluted and then filtered. On refluxing the mixture of HNO_3 and H_2SO_4 with pristine or unmodified CNFs (u-CNFs) defects were generated on the surface of u-CNF, which can serve as anchor groups for functionalization. The resultant residue was then washed with distilled water. But stirring for a prolong time can affect geometry and length of carbon nanofibers (CNFs). Therefore, a strong oxidizing agent, H_2O_2 was added to the processed u-CNFs for the generation of polar functionality by which it can be more compatible to polar epoxy. CNFs were allowed to react with strong oxidizing agent, H_2O_2/H_2SO_4 (volume ratio, 1:4) under constant stirring for 30 minutes at 70 ^oC. Addition of H_2O_2/H_2SO_4 to u-CNFs, introduced the polar functionality by which it could be more compatible to polar epoxy. To obtain the acid treated CNFs (t-CNFs), the final solution was centrifuged for several times in distilled water to remove the excess acid from the surface of t-CNFs.

2.3. Synthesis of epoxy/t-CNF Composites

The acid treated carbon nanofibers (t-CNFs) of different wt % (0.5, 1, 2, 3 and 4 wt %) were sonicated in acetone medium for 2 hr for better dispersion or to avoid agglomeration of t-CNF bundles. These well dispersed nanofibers were then added to the polymer epoxy resin and further sonicated for 3 hr followed by drying in vacuum oven for 24 hr to eliminate air bubbles. Then hardener (10 wt % of the epoxy resin) was added to the mixture by manual stirring for 10 minutes. Finally, it was casted into a mold and cured at open air for 48 hr. Same synthetic protocol was also adopted to fabricate epoxy nanocomposites with unmodified CNFs (epoxy/u-CNF nanocomposites).

2.4. Characterization of Materials

The surface morphology of epoxy/t-CNF nanocomposites was observed by SEM (model 5200, magnification x 30000, Jeol, Japan). The TEM (Tec-nai12, Philips, USA) of the samples was taken at 120 kV. FTIR spectra were recorded (Shimadzu IR Affinity-1 Fourier infrared spectrophotometer, Japan) in the range 400-4000cm-^{1}. XRD pattern were taken by an X-ray diffractometer (Rigaku, Japan, Model no. DD966) at 150 mA and 40 kV with Cu Kα (λ= 1.54 Å) radiation. The TGA (Model DTG-60, Shimadzu Corporation, Japan) measurement was done under nitrogen purge at a heating rate of 10 ^{o}C/min. A thin film of the sample was deposited on a mica surface to measure AFM using pico plus 5500 ILM AFM. The samples pressed into pellets, coated with silver paint on both surfaces and then conductivity was measured using LCR-Hi Tester (HOIKI, Japan, 3532-50) at ambient temperature. The mechanical properties were carried out by universal testing machine (Instron, UK, Model-5567) at a crosshead speed of 50 mm/min as per ASTM standard (D-638-00). All results were taken with an average of five samples of same composites.

3. Results and Discussion

3.1. FTIR analysis

The FTIR spectra of acid treated CNF (t-CNF), epoxy and epoxy/t-CNF nanocomposite are shown in Fig.1. Acid treated CNF (t-CNF) shows absorption bands at 3440 cm^{-1} and 1710 cm^{-1} associated to hydrogen bonded O-H stretching vibration and C=O stretching vibration in carboxylic acid (-COOH) groups respectively. The appearance of a peak at 1623 cm^{-1} is due to intermediate oxidation products, quinine groups [27]. The 1380 cm^{-1} peak results from the -OH

bending vibration from -COOH groups. For epoxy, two absorption bands at 3417 cm^{-1} and 1719 cm^{-1} are assigned to -OH stretching and carbonyl groups respectively. It is also observed that in FTIR spectra of composites, these bands shifted to lower wave numbers of 3343 $cm^{-1}$and 1711 cm^{-1}respectively in comparison to the epoxy. The shifting of FTIR peak from 3417 cm^{-1} to 3393 cm^{-1} is due to inter-molecular hydrogen bonding between t-CNF and epoxy linkages of epoxy resin. Besides the above two bands, the overall spectra of the composite appeared to be similar to that of epoxy. The results obtained in this present investigation are very similar to the results reported earlier [28].

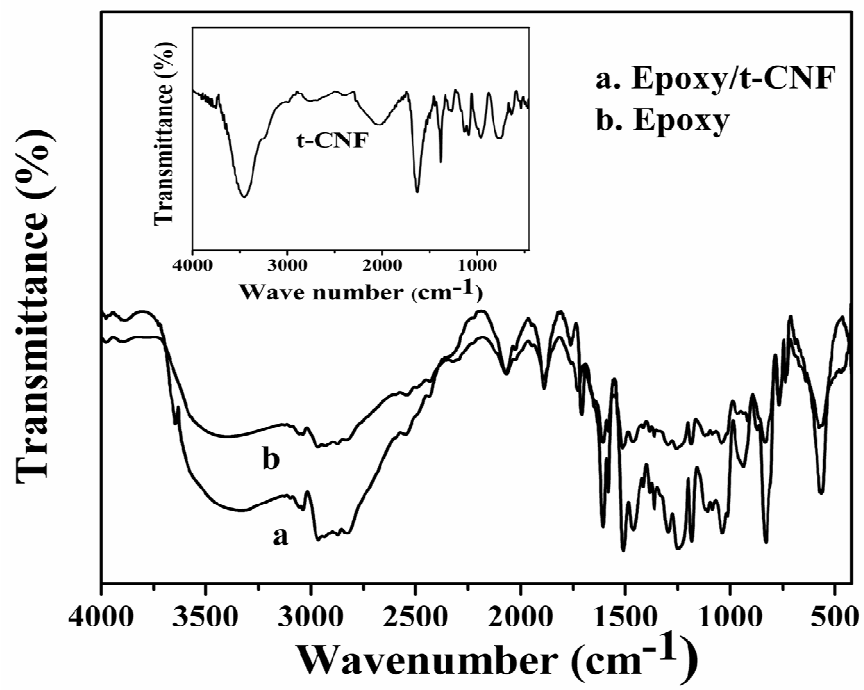

Fig.1. FTIR spectra of t-CNF (inset), epoxy and epoxy/t-CNF nanocomposites (4 wt %)

3. 2. XRD analysis

X-ray diffraction pattern of acid treated carbon nanofiber, t-CNF (Fig. 2 inset) shows a strong crystalline peak at $2\theta = 26^{o}$ is assigned to the (002) crystal plane of graphite [29] along

with another distinctive peak of graphitic nature at 2θ of 43.4^{o}. The XRD pattern of epoxy shows a broad peak centered at around 2θ≈19.5^{o}, indicating the amorphous nature of epoxy [30]. Nevertheless, all the epoxy/t-CNF nanocomposites with different t-CNF loading show a strong peak at 22.1^{o} with varying intensity. The upward shifting of the epoxy peak in epoxy/t-CNF nanocomposite clearly reveals a well dispersed phase of t-CNFs into epoxy resin which in turn influence the microstructure of the composite by means of interfacial interaction between the t-CNFs and epoxy matrix [31]. In other words, the characteristic crystalline peak of t-CNF is not in their initial position in epoxy nanocomposites as it is observed in case of t-CNF (inset Fig. 2) and it may be due to the broadening of the d-spacing of t-CNF by the epoxy matrix. It is also found that the intensity of the peak increases with the increase of t-CNF loading. It suggests that a crystalline phase is developed within the epoxy nanocomposites at higher wt % of t-CNF loading due to strong chemical interaction of t-CNFs and epoxy resin [31]. In other words, the upward shifting of the characteristic XRD peak may be accounted from the development of structural strain in epoxy nanocomposites. Such shifting in XRD peaks confirms the formation of epoxy/t-CNF nanocomposites via effective interfacial interaction between t-CNF and the epoxy matrix.

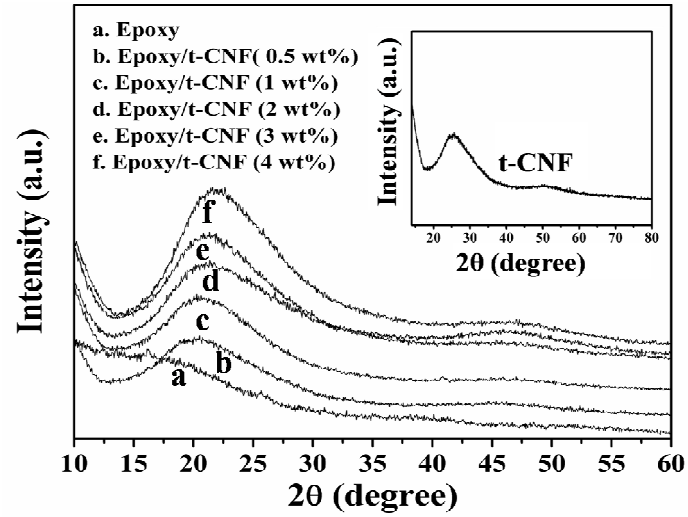

Fig.2. XRD pattern of t-CNF (inset), epoxy and epoxy/t-CNF nanocomposite at different weight percentage (wt %) of t-CNF.

3. 3. Morphological analysis

Fig. 3 shows the typical SEM images of the epoxy/t-CNF nanocomposites with different wt% of t-CNFs. Fig. 3a and 3b are the low-resolution SEM images of epoxy/t-CNF nanocomposites and reveals the crushed surfaces of this nanocomposite. From the high resolution image of this nanocomposite, t-CNFs are observed in the form of agglomeration as clusters or bundles with a diameter of about 10 µm (Fig.3c). The bundle acts as a stress concentration sites within the epoxy/t-CNF nanocomposites. In major portion of the SEM images, carbon nanofibers (t-CNFs) are dispersed homogeneously i.e. well separated and uniformly embedded in the resin matrix [24]. However, the t-CNFs in epoxy/t-CNF nanocomposites (3 wt %) show small aggregates with voids (Fig. 3d). These void numbers and size are gradually increased with increasing CNFs loading beyond 1wt%. The presence of voids in higher CNF loading due to filler aggregates indicates poorer dispersion [21]. Again, from the

TEM images of epoxy/t-CNF nanocomposites, a well dispersed phase of acid activated t-CNFs is observed at lower t-CNF content (Fig. 4a) , whereas; for higher wt% of t-CNF, a local agglomerating phase within the epoxy nanocomposite is observed. However, for higher t-CNF content (>1wt %), this surface activation stirred the carbon nanofibers to join and form larger aggregates (Fig. 4b) [33]. Moreover, the TEM micrograph in Fig. 4c indicated that in the process of making composites, the carbon nanofibers are broken due to intensive rolling [34].

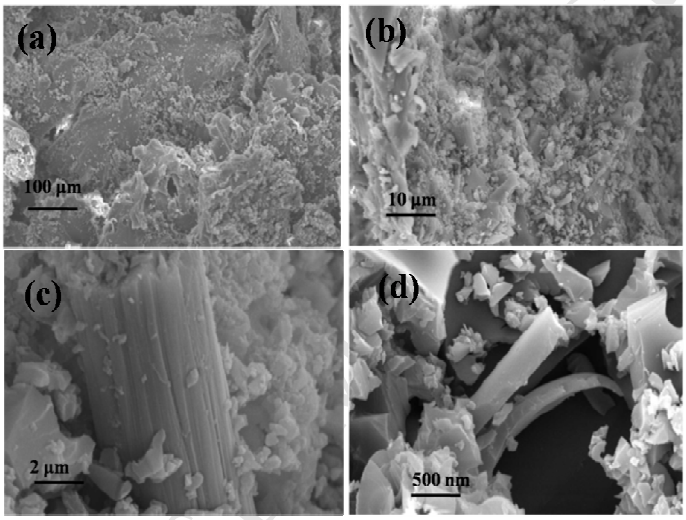

Fig.3. SEM of epoxy/t-CNF nanocomposites with (a) 0.5, (b) 1.0, (c) 2.0 and (d) 3.0 wt% of t-CNF.

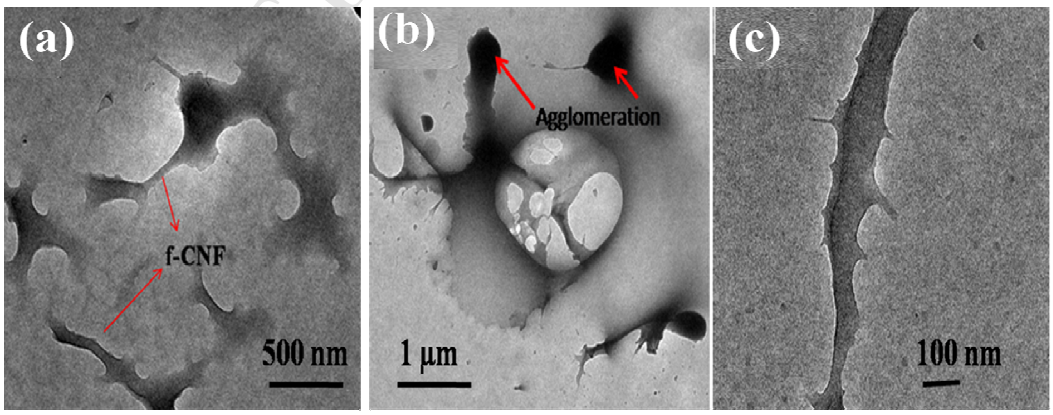

Fig.4. TEM images of epoxy/t-CNF nanocomposite (a) at 1wt% of t-CNF (b) 2wt% of t-CNF (c) after intensive rolling.

The compositional mapping with AFM is often used for the identification of multiple phases through color contrast. The brighter areas in the image can be attributed to the greater force experienced by the cantilever tip when it is in contact with the filler (tubular or spherical) whereas; dark patches appears when the tip is in contact with amorphous matrix state. Surface roughness can be calculated by measuring the height of the peak observed in the out of plane (z) direction. Fig. 5 shows the three dimensional AFM scans of fracture surfaces of the impact tested materials. The images are captured with a scan size that lines between 0.5 and 5 µm at the scan speed rate of 0.5 lines/sec. Images are processed by flatten using pico view 1.12 version software and manipulation has been done through pico-image advanced version software (Agilent technologies, USA). AFM image (Fig. 5a) of virgin epoxy reveals almost smooth surface, on the other hand, the images of epoxy nanocomposites show elevated peaks evidencing extremely rough surfaces caused by the presence of t-CNFs in the epoxy matrix. The average roughness of virgin epoxy (Fig. 5a) is found to be 1.18 nm whereas; the average roughness of the nanocomposite (Fig. 5b) in z direction is 10.52 nm for 4 wt% of t-CNF loading. It is due to the strong chemical interaction between the t-CNF and epoxy matrix.

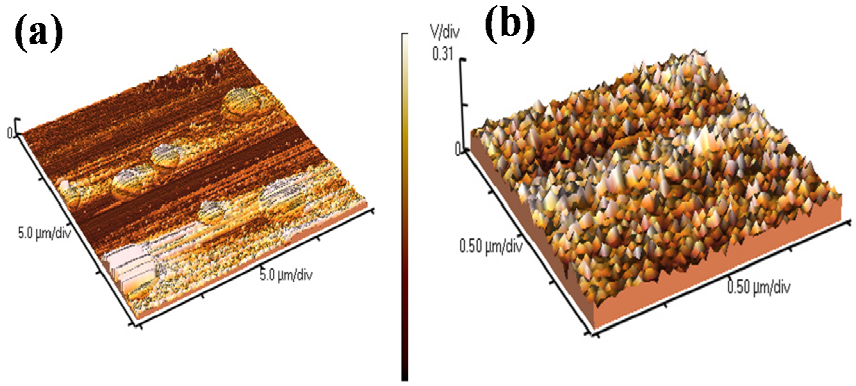

Fig.5. AFM images of **(a)** neat epoxy and **(b)** epoxy/t-CNF nanocomposite (4 wt %)

3.4. Thermal properties

Thermal properties of epoxy resin, t-CNF and epoxy/t-CNF nanocomposites are compared by thermogravimetric analysis (TGA) in the temperature range 50-700 ^{o}C under nitrogen atmosphere with a heating cycle of 10 ^{o}C/min (Fig. 6). The thermal decomposition of epoxy resin is occurred in three steps; (i) initial weight loss from 100 ^{o}C is due to the expulsion of water molecules from the surface of epoxy resin, (ii) another weight loss is observed at the temperature of 274 ^{o}C due to decomposition of epoxy resin, and (iii) the final weight loss is due to oxidation of partially decomposed epoxy resin in the temperature range of 600^{o}C. Fig. 6 demonstrates that the significant decomposition of all the epoxy/t-CNF nanocomposites is started at ≈ 290 ^{o}C and completed at ≈ 620, 640 and 655 ^{o}C for composites with 1, 2 and 3 wt % of t-CNFs respectively. In case of epoxy nanocomposites with 4 wt % of t-CNF, Fig. 6 shows the highest degree of thermal stability due to the shifting of 2nd and final decomposition temperature to higher side, i.e. 345 and 680 ^{o}C respectively. Thermal stability of the synthesized epoxy nanocomposites with reinforcement of t-CNF is found to increase with the increase in filler content. This retarding effect is attributed to incorporation of t-CNFs into epoxy matrix. This may be offering a stabilizing effect against the thermal decomposition of epoxy nanocomposites with reinforcement of acid treated carbon nanofibers (t-CNFs) [21]. Our present investigation shows that, acid treatment to pristine CNFs provides a better compatibility to epoxy matrix and thereby an excellent improvement in thermal stability due to uniform distribution of t-CNFs within epoxy/t-CNF nanocomposites. For the synthesized epoxy nanocomposites with 3 wt % of t-CNFs, a residue of about 18 % is observed to be left after complete thermal decomposition in the temperature range of 50^{o} to 700 ^{o} C, whereas; for the same filler loading in epoxy, i.e. 3 wt %

in the reported literature [25] shows a residue of ~ 10 % after thermal degradation in the temperature range of 30 ^{o} to 600 ^{o} C.

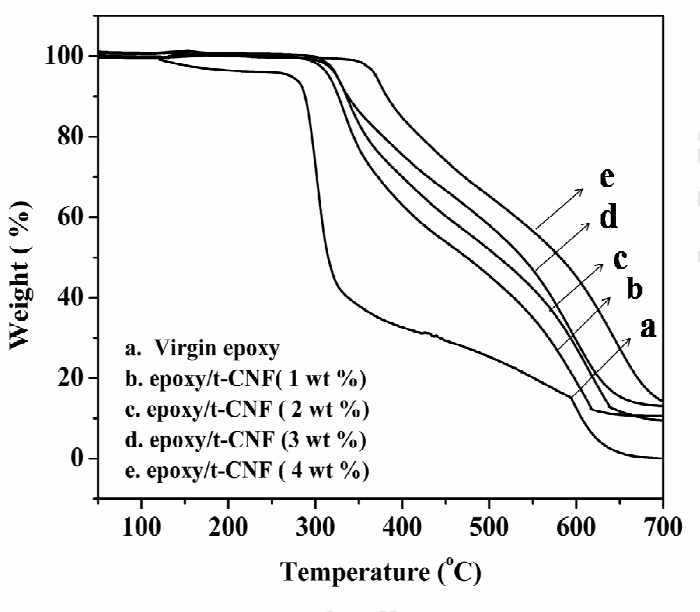

Fig.6. TGA curves of virgin epoxy and epoxy/t-CNF nanocomposites with different wt % of t-CNF.

3.5. Mechanical properties

Fig.7 shows the graphical presentation of tensile strength and Young's modulus of the epoxy nanocomposites as a function of their filler content, i.e. wt % t-CNF. The graph suggests an improvement of ≈ 3 % in strength and 6 % in modulus with addition of 0.5 wt% of t-CNF, whereas; 20 % and 19 % increment in strength and modulus are observed at 2 wt% of t-CNF. However, both the properties begin to degrade with further increase in t-CNF content. The present results are similar to the data reported by Choi et al. [21] during the study of carbon nanofiber reinforced epoxy nanocomposites. According to Choi et al., the maximum increase in tensile strength, i.e. 75 MPa is observed at 5 wt % of CNF loading, whereas; in present work

only 2 wt % of t-CNFs are observed to be efficient for the highest improvement, i.e. 47 MPa in tensile strength of the fabricated epoxy nanocomposites. Apparently the magnitude of tensile strength is appeared high for 5 wt % of CNF loading, but with respect to the amount of CNF loading it is very less as compared to our present work. The improvement in mechanical properties of t-CNF reinforced epoxy nanocomposite is highly affected by the nature of dispersion of the nanofibers. Stress concentration points are created due to agglomeration like impurities. More agglomeration is observed at higher wt % of t-CNF loading. The poor dispersion of carbon nanofibers within epoxy network leads to the weak improvement in mechanical properties. The presence of void may also be a reason for the degradation of mechanical properties. These voids are increased with the increase of t-CNF content. On the other hand, with increasing t-CNF content within the epoxy matrix, it causes a tremendous decrease in the plastic range of the epoxy matrix due to the development of crystalline phase within the nanocomposites, as evidenced from the XRD pattern. Due to such reason, ductility of the nanocomposites decreases and the brittleness increases with increasing filler content. A clear comparison of mechanical properties of acid treated CNF reinforced epoxy with respect to unmodified CNF has been drawn in Fig.7 and Fig.8. The change in mechanical properties of u-CNF/t-CNF reinforced epoxy nanocomposites with respect to the filler loading follows the same pattern, i.e. in both the cases a highest degree of improvement is achieved for 2 wt % of u-CNF/t-CNF loading. But the improvement is more pronounced for t-CNF as compared to u-CNF reinforced nanocomposites. This fact can be attributed from the better interfacial interaction improvised by the functional groups of acid treated CNF (t-CNF) and epoxy matrix. The expected improvement in mechanical properties of epoxy/u-CNF nanocomposite is hampered due to self assembling nature of unmodified CNFs at higher wt % of filler loading.

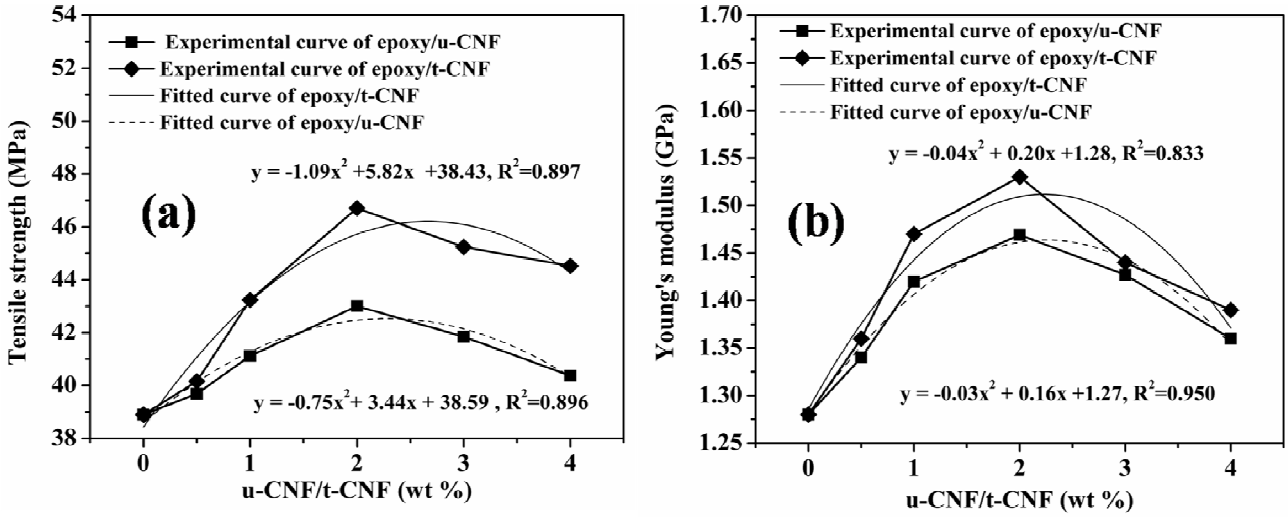

Fig.7. (a) Tensile strength and (b) Young's Modulus of modified and unmodified (t-CNF/u-CNF) reinforced epoxy nanocomposites.

The strain to failure (%) has been controlled for all samples during the tensile test. Further it has been seen that by adding more filler content into epoxy resin, strain to failure (%) decreases (Fig.8). This indicates that addition of filler to the epoxy resin makes the composite as brittle. The movement of polymer chains arrested due to addition of t-CNF filler makes the composite more brittle and stiffer [35]. Moreover, at higher loading of t-CNFs, inconvenient cracks are generated within the nanocomposites and propagated along the weak t-CNF and epoxy interface. Hence, the optimum care should be taken for the uniform dispersion of t-CNF within epoxy matrix so that the improvement of the mechanical properties will not be hampered. Similar type of result has been reported by Zhou et al. [25] for vapor grown carbon nanofiber reinforced epoxy nanocomposites.

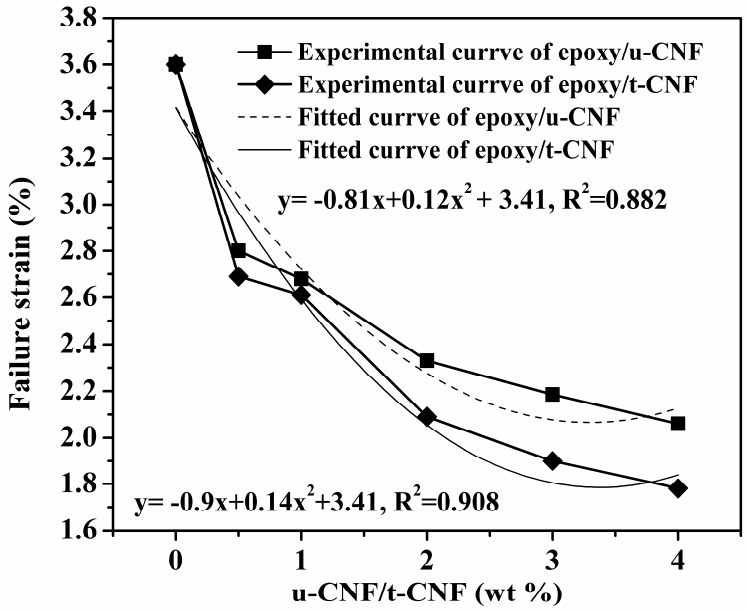

Fig.8. Failure strain (%) vs. filler content of modified and unmodified (t-CNF/u-CNF) reinforced epoxy nanocomposites

3.6. Electrical properties

Fig.9 shows the variation in electrical conductivity of epoxy/t-CNF and epoxy/u-CNF nanocomposites with increasing t-CNF/u-CNF content. It is found that the electrical conductivity of epoxy nanocomposite increases with increase in filler content. The conductivity of epoxy nanocomposites is found to be improved by 3 orders of magnitude with just 0.5wt % of t-CNF loading within epoxy matrix. However, it is interesting to notice that a sharp increase of about nine orders in conductivity from 0.5wt % to 1.0 wt % of t-CNF. This indicates that the percolation threshold is reached at 1.0 wt % of t-CNF for the nanocomposites. It is also observed that after the threshold point, addition of more and more t-CNFs (2 wt %, 3 wt % and 4 wt %) within epoxy network has a very poor impact on the electrical conductivity of nanocomposites [25]. The expected increase in electrical conductivity of epoxy/t-CNF nanocomposites at higher loading level may be hampered due to the agglomeration of t-CNF within the host epoxy matrix.

This reveals that, the chemical modification of CNF causing improved nanofiber dispersion and helped the formation of conductive network within the epoxy matrix with a significant increase in electrical conductivity of epoxy/t-CNF nanocomposites at lower range of t-CNF [36]. In case of u-CNF reinforced epoxy nanocomposite (epoxy/u-CNF), the electrical conductivity is found to increase with increase in u-CNF content, but the value of conductivity is much lower as compared to acid treated CNF (t-CNF) reinforced epoxy nanocomposites. This can be explained from the high tendency of self agglomeration of unmodified carbon nanofibers (u-CNFs). Due to such reason a highly connected conductive network is not achieved for epoxy/u-CNF nanocomposites, as it is seen for epoxy/t-CNF nanocomposites. The improved electrical conductivity for epoxy/t-CNF nanocomposite reveals the better interfacial interaction between acid treated CNFs (t-CNFs) and epoxy as compared with the unmodified CNFs. Same type of result has been reported by Choi et al.[21], where interpretation of electrical conductivity is carried out in terms of decreasing electrical resistivity.

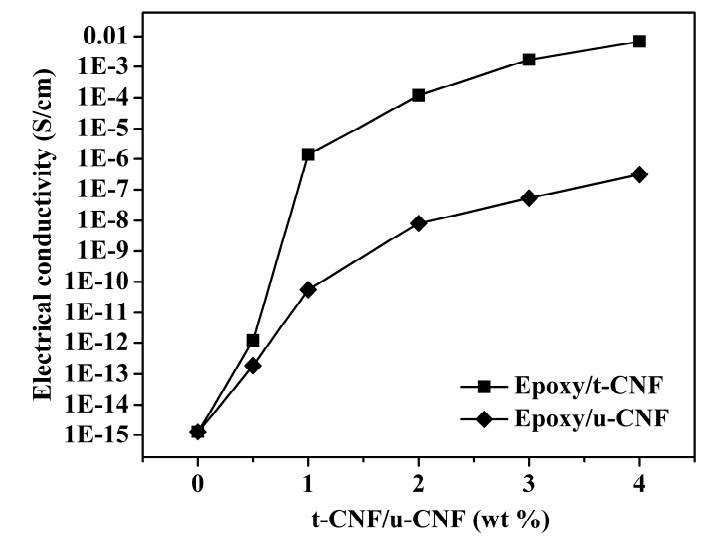

Fig.9. Electrical conductivity of the epoxy/t-CNF nanocomposites at different wt% of t-CNF

4. Conclusion

Acid treated carbon nanofiber (t-CNF) reinforced epoxy nanocomposites are synthesized by hand lay-up method and before processing, non polar or pristine CNFs (u-CNFs) are made compatible with epoxy matrix via acid treatment. The compatibility of nonpolar filler like CNF and polar matrix like epoxy is a challenge for making epoxy nanocomposites with improved properties. Mixed acid treatment on pristine CNFs is employed to introduce functional groups on the surface of carbon nanofibers (t-CNFs) and to improve the interfacial interaction between carbon nanofiber and epoxy matrix. The conversion of u-CNF to t-CNF is confirmed through the FTIR analysis of t-CNF. The synthesized epoxy/t-CNF nanocomposites are characterized by XRD, FTIR, SEM and TEM whereas; the surface topology is investigated by AFM study. The synthesized material is found to have high thermal, mechanical and electrical properties. The improvement in mechanical properties is more pronounced for acid treated CNFs (t-CNFs) with respect to the unmodified CNFs (u-CNFs). For epoxy/t-CNF nanocomposites, tensile strength and Young's modulus are increased up to 20 % and 19 % at 2 wt % of t-CNF loading. The decreasing pattern of strain to failure (%) is attributed by the brittle nature of epoxy/t-CNF with incorporation of higher wt % of t-CNF to the epoxy matrix. With a very little amount of the t-CNFs (0.5- 1 wt %), an inter-connecting conducting network is formed within epoxy resin resulting a sharp rise in electrical conductivity of epoxy/t-CNF nanocomposite. This work may contribute to tailoring of high performance epoxy composites with desired thermal, mechanical and electrical properties.

Acknowledgement

Authors express their thanks to Department of Science and Technology, Government of Odisha, India for financial support (ST-BIO-15/2014/ST/2014).

References

[1] X. Huang, Materials 2 (2009) 2369–2403.

[2] C. Xiang, N. Behabtu, Y. Liu, H.G. Chae, C.C. Young, B. Genorio, J.M. Tour, ACS Nano. 7 (2013) 1628–1637.

[3] W. Lu, M. Zu, J.H. Byun, B.S. Kim, T.W. Chou, Adv. Mater. 24 (2012) 1805–1833.

[4] S. Chand, J. Mater. Sci. 35(2000) 1303–1313.

[5] J.L. Vilaplana, F.J. Baeza, O. Galao, E. Zornoza, P. Garcés, Materials 6 (2013) 4776–4786.

[6] F.J. Baeza, O. Galao, E. Zornoza, P. Garcés, Materials 6 (2013) 841–855.

[7] Z. Fan, J. Yan, T. Wei, L. Zhi, , G. Ning , T. Li, F. Wei, Adv. Funct. Mater. 21(2011) 2366-2375.

[8] Z. Wangxi, L. Jie, W. Gang, Carbon 41 (2003) 2805–2812.

[9] V. Kuzmenko, O. Naboka, H. Staaf, M. Haque, G. Göransson, P. Lundgren, P. Enoksson, Mater. Chem. Phys. 160 (2015) 59-65.

[10] K. Chen, X. Huang, C. Wan, H. Liu, Mater. Chem. Phys. 164 (2015) 85-90

[11] L. Guadagno, M. Raimondo, V. Vittoria, L. Vertuccio, K. Lafdi, B.D. Vivo, P. Lamberti, P. Spinelli, V. Tucci, Nanotechnology 24 (2013) 305704.

[12] L.H. Sun, Z. Ounaies, X.L. Gao, C. A. Whalen, Z. G. Yang, J. Nanomater. 2011 (2011) 1-8.

[13] V.Z. Mordkovich, Theor. Found. Chem. Eng. 37 (2003) 429-438.

[14] A. Allaoui, S.V. Hoa, M.D. Pugh, Compos. Sci. Technol. 68 (2008) 410-416.

[15] D. Puglia, L. Valentini, J.M. Kenny, J. Appl. Polym. Sci. 88 (2003) 452–458.

[16] Y.H. Chang, K.F. Lin, Mater. Chem. Phys. 173(2016) 446-451.

[17] M. S. Goyat, S. Suresh, S. Bahl, S. Halder, P.K. Ghosh, Mater. Chem. Phys. 166 (2015). 144-152.

[18] S. Bal, Mater. Des. 31 (2010) 2406-2413.

[19] K.J. Green, D. R. Dean, U. K. Vaidya, E. Nyairo, Compos. Part A: Appl. Sci. Manuf. 40 (2009) 1470-1475.

[20] R.D. Patton, C.U. Pittman, L. Wang, J.R. Hill, Compos. Part A: Appl. Sci. Manuf. 30 (1999) 1081-1091.

[21] Y.K. Choi, K.I. Sugimoto, S.M. Song, Y. Gotoh, Y. Ohkoshi, M. Endo, Carbon 43 (2005) 2199-2208.

[22] J. Sandler, P. Werner, M.S.P. Shaffer, V. Demchuk, V. Altstadt, A.H. Windle, Compos. Part A: Appl. Sci. Manuf. 33 (2002) 1033-1039.

[23] H. Ma, J. zeng, M.L. Realff, S. Kumar, D.A. Schiraldi, Compos. Sci. Technol. 63 (2003) 1617-1628.

[24] Y.K. Choi, K.I. Sugimoto, S.M. Song, M. Endo, Mater. Lett. 59 (2005) 3514-3520.

[25] Y. Zhou, F. Pervin, S. Jeelani, J. Mater. Sci. 42 (2007) 7544-7553.

[26] J. Zhu, S. Wei, J. Ryu, M. Budhathoki, G. Liang, Z. Guo, J. Mater. Chem. 20 (2010) 4937-4948.

[27] T. A. Saleh, V. K. Gupta, Nanomaterial and Polymer Membranes: Synthesis, Characterization, and processing, First Ed., Amsterdam, Netherlands (2016)115

[28] A.K. Pradhan, S.K. Swain, Iran. Polym. J. 22 (2013) 369-376.

[29] L. Zhang, A. Aboagye, A. Kelkar, C. Lai, H. Fong, J. Mater. Sci. 49 (2014) 463–480.

[30] S. Swarup, Mater. Sci. Appl. 2 (2011) 1516-1519.

[31] Z. Wang & G. L. Zhao, Open J. Compos. Mater.3 (2013) 17-23.

[32] F. Pervin, Y. Zhou, V.K. Rangari, S. Jeelani, Mater. Sci. Eng. A. 405 (2005) 246-253.

[33] S.G. Prolongo, M. Campo, M.R. Gude, R. Chaos-Morán, A. Ureñ, Compos. Sci. Technol. 69 (2009) 349-357.

[34] G.H. Chen, D-J. Wu, W-G, Weng, B. He, W-L Yan, Polym. Int. 50 (2001) 980-985.

[35] M. M. Shokrieh, M. Esmkhani, F. Vahedi, H. R. Shahverdi, Iran. Polym. J. 22 (2013) 721-727.

[36] J.J. Karippal, H.N. Narasimha Murthy, K.S. Rai, M. Krishna, M. Sreejith, Polym. Bull. 65 (2010) 849-861.

Figure Captions

Fig.1. FTIR spectra of t-CNF (inset), epoxy and epoxy/t-CNF nanocomposites (4 wt %).

Fig.2. XRD pattern of t-CNF (inset), epoxy and epoxy/t-CNF nanocomposite at different weight percentage (wt %) of t-CNF.

Fig. 3 SEM of CNF/ epoxy nanocomposite: (a) 0.5, (b) 1, (c) 2 and (d) 3 wt% of t-CNF.

Fig. 4 TEM images of epoxy/ t-CNF nanocomposite (a) at 1wt% of t-CNF (b) 2wt% of t-CNF (c) after intensive rolling.

Fig. 5 AFM images of **(a)** neat epoxy and **(b)** epoxy/t-CNF nanocomposite (4 wt %)

Fig. 6 TGA curves of virgin epoxy and epoxy/t-CNF nanocomposites with different wt % of t-CNF.

Fig. 7(a) Tensile strength and **(b)** Young's Modulus of modified and unmodified (t-CNF/CNF) reinforced epoxy nanocomposites.

Fig.8 Failure strain (%) vs. filler content of modified and unmodified (t-CNF/CNF) reinforced epoxy nanocomposites

Fig.9 Electrical conductivity of the epoxy/t-CNF nanocomposites at different wt% of t-CNF

Highlights

Title: " Design of carbon nanofiber embedded conducting epoxy resin"

- Epoxy/t-CNF nanocomposites are characterized by XRD, FTIR, SEM, AFM and TEM.
- Electrical conductivity was achieved by epoxy with a threshold at 1 wt% of t-CNF.
- Tensile strength is enhanced by 40% due to dispersion of t-CNF.
- Synthesized nanocomposites are suitable for fabricating electronic devises.